



Latency of chromatic information in area V4



Mindy Chang^a, Sherry Xian^b, Jonathan Rubin^c, Tirin Moore^{b,*}

^a Department of Bioengineering, Stanford University, Stanford, CA, USA

^b Department of Neurobiology, Stanford University, Stanford, CA, USA

^c Interdisciplinary Center for Neural Computation, Hebrew University, Jerusalem, Israel

ARTICLE INFO

Article history:

Available online 27 June 2013

Keywords:

Color vision
Parallel visual pathways
Koniocellular
Equiluminance
Ventral visual cortex
S-cone
L/M-cone

ABSTRACT

In the primate visual system, information about color is known to be carried in separate divisions of the retino-geniculate-cortical pathway. From the retina, responses of photoreceptors to short (S), medium (M), and long (L) wavelengths of light are processed in two different opponent pathways. Signals in the S-opponent pathway, or blue/yellow channel, have been found to lag behind signals in the L/M-opponent pathway, or red/green channel in primary visual area V1, and psychophysical studies have suggested similar perceptual delays. However, more recent psychophysical studies have found that perceptual differences are negligible with the proper controls, suggesting that information between the two channels is integrated at some stage of processing beyond V1. To study the timing of color signals further downstream in visual cortex, we examined the responses of neurons in area V4 to colored stimuli varying along the two cardinal axes of the equiluminant opponent color space. We used information theory to measure the mutual information between the stimuli presented and the neural responses in short time windows in order to estimate the latency of color information in area V4. We found that on average, despite the latency difference in V1, information about S-opponent signals arrives in V4 at the same time as information about L/M-opponent signals. This work indicates a convergence of signal timing among chromatic channels within extrastriate cortex.

© 2013 Elsevier Ltd. All rights reserved.

1. Introduction

Color vision is a fundamental aspect of visual processing that is closely related to the perception of form, as colors help to define borders and facilitate object recognition. In the primate visual system, anatomical and physiological evidence suggests that information about color and form are carried in separate divisions of the retino-geniculate-cortical pathway (Wiesel and Hubel, 1966; Derrington et al., 1984; De Valois et al., 2000; Chatterjee and Callaway, 2003). However, the degree to which the pathways are parallel in each area remains controversial.

The retina contains three classes of photoreceptors, called S, M, and L cones, that respond to overlapping wavelengths of light, with peaks at short (S, blue), medium (M, green), and long (L, red) wavelengths respectively. Each cone is color-blind, responding only to the level of activation, and unable to distinguish between changes in intensity and changes in wavelength. As the cone activation signals are passed to the lateral geniculate nucleus (LGN) in the thalamus, they are processed in opponent pathways: two chromatic pathways, and an achromatic pathway. The two chromatic path-

ways are S – (L + M) (the difference between S-cone activation and the sum of L- and M-cone activation, also known as the blue/yellow channel or S-opponent pathway) and L – M (the difference between L- and M-cone activation, also known as the red/green channel or L/M opponent pathway). S-opponent signals are carried predominantly in the koniocellular layers of LGN, while the L/M-opponent signals are carried in the parvocellular layers of the LGN. The third achromatic channel, which contains luminance signals (L + M), is carried in the magnocellular layers of the LGN. In the cortex, color signals are passed along the ventral pathway from primary visual area V1–V2, V4, and TE. Within each of these areas, studies have shown clustering of color-selective regions. Color selective regions are concentrated in blobs in V1 (Livingstone and Hubel, 1984) and thin stripes in V2 (Hubel and Livingstone, 1987), as revealed through cytochrome oxidase staining for metabolic activity. There is also evidence that processing of different features is integrated early on in the visual system (Sincich and Horton, 2005). Recent fMRI, optical imaging, and electrophysiological work have found color-selective regions, or 'globes', within area V4 (Conway et al., 2007; Tanigawa et al., 2010; Kotake et al., 2009).

In order to create a percept of color and form, the information from separate channels must be integrated at some stage of processing. Several studies have suggested that the S-opponent pathway is slow compared to the L/M-opponent and luminance pathways. In particular, a study by Cottaris and Devalois found that

* Corresponding author. Address: 299 Campus Drive West, Room D200, Stanford, CA 94305-5125, USA. Tel.: +1 (650) 725 8712; fax: +1 (650) 725 3958.

E-mail address: tirin@stanford.edu (T. Moore).

in primary visual area V1, the S-opponent pathway is slow compared to the L/M opponent pathway, with a delay of about 30 ms (Cottaris and De Valois, 1998). Although morphological and functional differences have been observed between the S-opponent and L/M-opponent pathway earlier in the visual pathway, no concrete evidence has been found for differences in latency at the level of the receptors in the retina (Schnapf et al., 1990), ganglion cells (Yeh et al., 1995), or LGN (Tailby et al., 2008). Psychophysical studies have also suggested that the perception of S-cone signals is sluggish compared to other channels, but evidence for this is weak once controls for behavioral readout and adaptation are taken into account (see Section 4).

An examination of brain regions beyond V1 could provide insight into the temporal properties and degree of integration between the two chromatic pathways. In this study, we used information theory to measure the mutual information between short segments of the neural responses and the color of the stimulus presented in order to estimate the latency of color information in area V4. We presented a series of short bar flashes within the RF of single neurons recorded in area V4, varying color along the two cardinal axes of the equiluminant opponent color space. Despite the latency difference in V1, we found that on average, information about S-opponent signals arrives in V4 at the same time as information about L/M-opponent signals.

2. Materials and methods

2.1. Subjects

We recorded the responses of single V4 neurons in two adult male rhesus monkeys (*Macaca mulatta*, 5–10 kg) using standard neurophysiological methods. General experimental and surgical procedures have been described previously (Graziano et al., 1997). Each animal was surgically implanted with a head post, a

scleral eye coil, and recording chambers. Surgery was conducted using aseptic techniques under general anesthesia (isoflurane) and analgesics were provided during post-surgical recovery. All experimental procedures were in accordance with National Institutes of Health Guide for the Care and Use of Laboratory Animals, the Society for Neuroscience Guidelines and Policies, and Stanford University Animal Care and Use Committee.

2.2. Visual stimuli

All stimuli were presented on a colorimetrically calibrated CRT display (Mitsubishi 2070SB-BK, 29 cm vertical and 39 cm horizontal, 60 Hz) controlled by a Pentium-based computer with an NVIDIA FX5200 video card (8 bits per gun). Judd chromaticities of the phosphors were measured with a Photo Research PR-650 SpectraColorimeter and the output of each phosphor was linearized using an International Light IL1700 Radiometer (Judd, 1951). The values were Red (0.628,0.342), Green (0.294,0.612), and Blue (0.152,0.081). Stimuli were chromatic, oriented bars ($1 \times 0.25^\circ$ of visual angle) presented on the neutral gray background and centered in the RF of individual V4 neurons (Fig. 1A). Orientation of the bar was 0° , 45° , 90° , or 135° , pre-determined during the RF mapping.

The luminance of all bar colors was held constant at 25 cd/m^2 , an increment to the background luminance which was fixed at 15 cd/m^2 . In natural scenes, differences in color are usually associated with differences in luminance, and increases in luminance have been found to facilitate detection of chromatic stimuli (Eskeew Jr et al., 1994; Cole et al., 1990). Luminance was corrected for individual monkeys using methods described below. The chromaticities of the stimuli were specified in a color space based on opponent representation of cone responses (MacLeod and Boynton, 1979). Cone excitations were calculated using Smith–Pokorny cone fundamentals based on human observers (Smith and Pokorny, 1975). This color space is similar to the one proposed by MacLeod

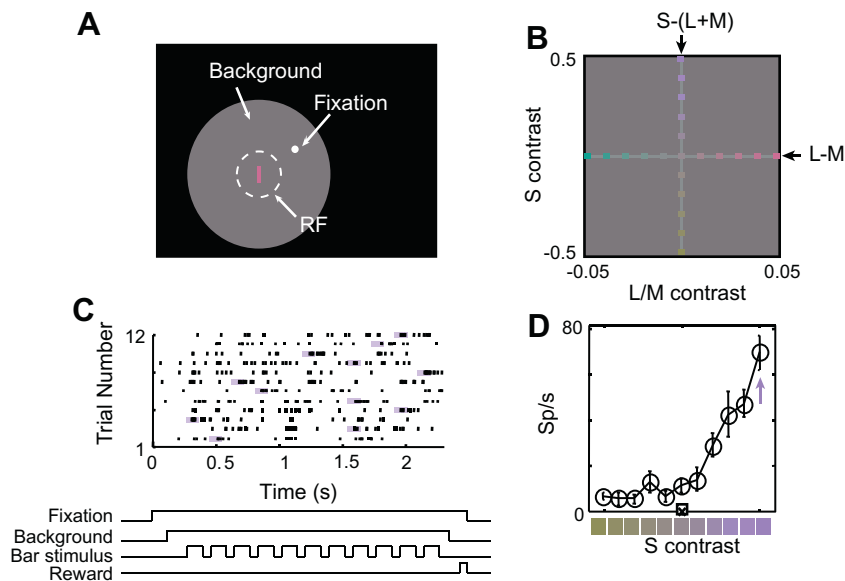


Fig. 1. Experimental setup: color stimuli and example recording. (A) Layout of visual stimulation. In this passive viewing task, the monkey maintained fixation on a white dot while a gray EES (Equal Energy Spectrum, $L - M = 0.665$, $S - (L + M) = 1.02$, 25 cd/m^2) background and colored, oriented bar stimuli were flashed in the center of the mapped response field (RF) of a single V4 neuron. (B) Contrast stimulus space. The tested contrasts were distributed along orthogonal axes, based on the normalized MacLeod–Boynton equiluminant chromaticity space. S contrasts ranged from -0.5 to 0.5 , while L/M contrasts ranged from -0.05 to 0.05 relative to EES. (C) Timing of stimulus presentation. Once fixation was acquired, a gray EES background appeared followed by a pseudorandom sequence of 11 colors along one of the two contrast axes. Each stimulus lasted 100 ms followed by a 83 ms of the EES background. Within a trial, each contrast was presented only once. The example raster shown shows tick marks for each spike within each trial across time, with highlighted boxes indicating the time windows in which the 0.5 S contrast stimulus was presented. (D) Example tuning curve, based on part C. Average spike rate responses are plotted as open circles for each contrast level with error bars indicating SEM. The open square denotes the mean response to the EES background and the cross denotes the spontaneous activity.

and Boynton (1979) and used by Derrington et al. (1984) but specifies chromaticities in terms of contrasts with respect to a neutral gray. The two coordinate axes of this color space correspond to L- versus M-cone (denoted by L – M axis) and S- versus L- and M- cone (S – (L + M) axis), normalized by L + M (luminance axis). L and M variations along the L – M axis are antagonistic such that the sum of L and M cone excitations is constant, and contrast is measured as the difference of L and M cone contrasts, i.e., positive values correspond to increasing L- and decreasing M-cone excitation. Positive values on the S – (L + M) axis correspond to positive S-cone contrast (MacLeod and Boynton, 1979). Each bar had different L – M or S – (L + M)) contrasts relative to an Equal Energy Spectrum (EES) reference color (Judd $(x,y) = (0.333,0.333)$, 25 cd/m²). Chromatic contrast was specified using Michelson contrast. Because of the gamut limit of the CRT monitor, cone contrasts in the L – M axis varied from –0.05 to 0.05 and contrasts in the S – (L + M) axis varied from –0.5 to 0.5. Equivalent Weber contrasts were from –0.1 to 0.1 for L – M axis and from –0.7 to 2.0 for S – (L + M) axis. V4 neurons were tested along the cardinal cone contrast axes. 11 contrasts were picked along the L – M axis with zero contrast in S and another 11 contrasts were similarly picked along the S – (L + M) axis (Fig. 1B).

A minimum motion technique was used to determine equiluminance for each monkey using the method of Logothetis and Charles (1990). In this paradigm, four horizontal square-wave gratings (4°) were displayed sequentially and repeatedly for 1 s. Spatial and temporal frequencies were 1 cycles/° and 3 cycles/s, respectively. The gratings were superimposed and each grating was displaced by one-quarter cycle from the previous one. The first and third gratings were composed of chromatic stripes, whose colors were composed of two of the three monitor phosphors (red/green, red/blue or green/blue). Luminance of one phosphor was fixed at 13 cd/m² and luminance of the other phosphor varied between 8.5 cd/m² and 17.5 cd/m² at 10 different levels. The second and fourth gratings were composed of light and dark stripes, whose chromaticity was the mixture of the used two phosphors in the chromatic gratings. The mean luminance of these gratings was constant at the mean luminance level of the two chromatic ones, and of a fixed 10% contrast. The sequence of stimuli resulted in an apparent motion (drifting upward or downward) when the luminance of the two colors in the chromatic gratings was not perceived as equal. When monkeys were trained to fixate within the grating stimuli, optokinetic nystagmus was readily elicited when the luminance contrast of the two chromatic gratings differed perceptually. Because the eye drift reversed upon crossing a particular luminance contrast when the two component colors in the chromatic grating were perceived equally bright, direction of the slow phase of the nystagmus for the various luminance contrasts gave reliable estimates of equiluminant points for each monkey.

2.3. Behavioral task

Monkeys were seated in a primate chair in a quiet room and secured with a surgically implanted head post, and positioned 57 cm in front of a CRT monitor. Each monkey was trained to fixate a central spot (0.1°, 50 cd/m²) on the CRT display where visual stimuli were presented. Their gaze remained within a 1–1.2° fixation window through all trials. During each experimental trial, monkeys fixated the central point for 2.5 s to receive a juice reward. Two hundred and fifty milliseconds after fixation began, a circular neutral gray background (16°) appeared in the lower contralateral quadrant and remained until the end of the trial. One hundred and fifty milliseconds following the appearance of the gray background, a pseudorandom sequence of 11-color contrast bar stimuli was presented in the RF of the neuron under study (Fig. 1A). Each bar stimulus lasted 100 ms and was followed by 50 ms of the neu-

tral gray background (Fig. 1C). Monkeys were required to maintain fixation throughout the course of visual stimulus presentation and only correctly completed trials were included in the analyses. Eye position was monitored via a scleral search coil, digitized and stored at 200–500 Hz. Stimulus presentation, data acquisition and behavioral monitoring were controlled by the CORTEX system.

2.4. Data analysis

All analyses were performed in Matlab (Mathworks).

2.4.1. Mutual information

We used mutual information (MI) to determine the selectivity of V4 neurons for color. MI offers a way to quantify the association between two random variables (Cover and Thomas, 1991), in this case, between the stimuli and responses. More specifically, MI measures the degree to which knowledge of one variable can reduce uncertainty about the other. Formally, given a set of stimuli S (e.g., colors) and responses \mathcal{R} (e.g., spike counts), the MI takes the following forms:

$$I(R; S) = \sum_{s \in S} \sum_{r \in \mathcal{R}} p(r, s) \log_2 \left(\frac{p(r, s)}{p(r)p(s)} \right) \quad (1)$$

$$= \sum_{s \in S} p(s) \sum_{r \in \mathcal{R}} p(r|s) \log_2 \left(\frac{p(r|s)p(s)}{p(r)p(s)} \right) \quad (2)$$

$$= - \sum_{r \in \mathcal{R}} p(r) \log_2 p(r) + \sum_{s \in S} p(s) \sum_{r \in \mathcal{R}} p(r|s) \log_2 p(r|s) \quad (3)$$

$$= H(R) - H(R|S) \quad (4)$$

where S and R are the stimuli and responses respectively, $p(r, s)$ is the joint distribution of the presented stimuli and responses, and $p(r|s)$, $p(r)$, and $p(s)$ are the corresponding conditional and marginal distributions. The base of the logarithm (taken as 2) specifies that information is measured in bits. Finally, $H(\cdot)$ denotes the entropy of a random variable. Entropy measures the amount of uncertainty in a random variable (Cover and Thomas, 1991):

$$H(X) = - \sum_{x \in \mathcal{X}} p(x) \log_2 p(x) \quad (5)$$

$$H(X|Y) = - \sum_{y \in \mathcal{Y}} p(y) \sum_{x \in \mathcal{X}} p(x|y) \log_2 p(x|y) \quad (6)$$

Thus, $I(R; S)$ here quantifies the degree to which the entropy (or uncertainty) of an observed neural response $H(R)$ is reduced given knowledge about the presented stimulus $H(R|S)$. This framework allows us to directly compare the color selectivity across S and L/M stimuli as well as across individual neurons.

2.4.2. Estimating MI from the data

We analyzed the neural responses to the color bar stimuli, considering each of the two cardinal axis of color contrasts (S and L/M) separately. Thus, the stimuli S consisted of $n = 11$ colors within each analysis. The response variable $R \in \{0, 1, 2, \dots\}$ was taken as the spike counts in a 15 ms sliding window following stimulus onset in individual trials, and trials from all orientations were pooled for a more robust estimation of the MI. To estimate $I(R; S)$, we calculated the empirical joint distribution $\hat{p}(r, s)$ by counting the number of occurrences of each possible response for each stimulus across the different presentation trials. We then calculated an estimate of $I(S; R)$ using this empirical distribution as specified in Eq. (1). This resulted in an estimate for the MI between a short time bin of the neural response and the stimulus color presented. Finally, we repeated the analysis for each time window, shifting by 5 ms at each step from the onset of the stimulus to the onset of the subsequent stimulus.

2.4.3. Bias correction

Given the stochastic nature of neural spiking and a finite sample of neural responses to each stimulus (due to a limited number of experimental trials), the empirical joint probability distribution $\hat{p}(r, s)$ can sometimes be a poor estimate of the actual underlying distribution $p(r, s)$. The amount of bias in MI estimation depends on how densely the joint distribution matrix is sampled. As MI is constrained to be a positive number, the information calculation incurs a positive bias from the finite sample size, creating an overestimate of the actual MI value. The amount of bias can be approximated as a function of the number of bins in the joint distribution and the total number of trials (Panzeri and Treves, 1996). One possible solution to the problem of overfitting and bias is to reduce the details of the stimulus and response descriptors such that their joint distribution can be better estimated. To correct for the bias, we used the algorithm developed by Nelken et al. (2005) in which the MI was calculated based on successively reduced representations of the joint distribution matrix. At each step, the row or column with the least marginal probability is selected and joined to the neighbor that has the lower marginal probability. The MI of the reduced matrix and the estimated bias are computed, generating a sequence of bias-corrected MI estimates. The corrected MI was taken as the maximum bias-subtracted value across all estimates of the joint distribution (Nelken and Chechik, 2007), providing a conservative estimate of the actual MI. To test for significance, we also controlled for bias by using a shuffled bootstrap method (Efron, 1979). For each MI calculation, the pairing of stimuli and responses were shuffled across all flash presentations and recalculated 100 times to find a null distribution for the MI values. For a given time point, if the MI exceeded the maximum of the bootstrap values, the MI was taken to be significant with $p < 0.01$.

2.4.4. Latency estimation

In order to determine the latency with which chromatic information emerged in individual neurons, we considered the timecourse of the MI compared to the bootstrap distribution. In order to reduce artifacts, we imposed a relatively strict heuristic to determine the latency of information. The first of five consecutive time points in which the MI exceeded the maximum of the bootstrap values was taken as the latency. This was done to avoid selecting spurious time points at which the MI exceeded the bootstrap value. This method of latency estimation is similar to measures that have been used in determining the timecourse of motion detection in MT neurons (Osborne et al., 2004). Consecutive bins of significantly elevated spiking activity compared to baseline have also been used to quantify onset latencies of neural responses (Schmolesky et al., 1998).

2.4.5. Controls for robustness of MI measure

We calculated the MI in sliding time windows and examined the effect of changing the size of the analysis window. We also examined the MI using accumulating time windows, where each window included all preceding spikes back to the onset of the stimulus. However the information timecourse had poorer time resolution than that of the short sliding analysis windows, possibly due to noise from the baseline firing.

3. Results

We studied the visual responses of 255 single V4 neurons to colored bar stimuli in two monkeys (217, monkey B; 38, monkey W). Fig. 1D shows a tuning function for an example neuron across S contrast stimuli, as measured by the spike rate in a 100 ms window following the stimulus onset. This particular neuron

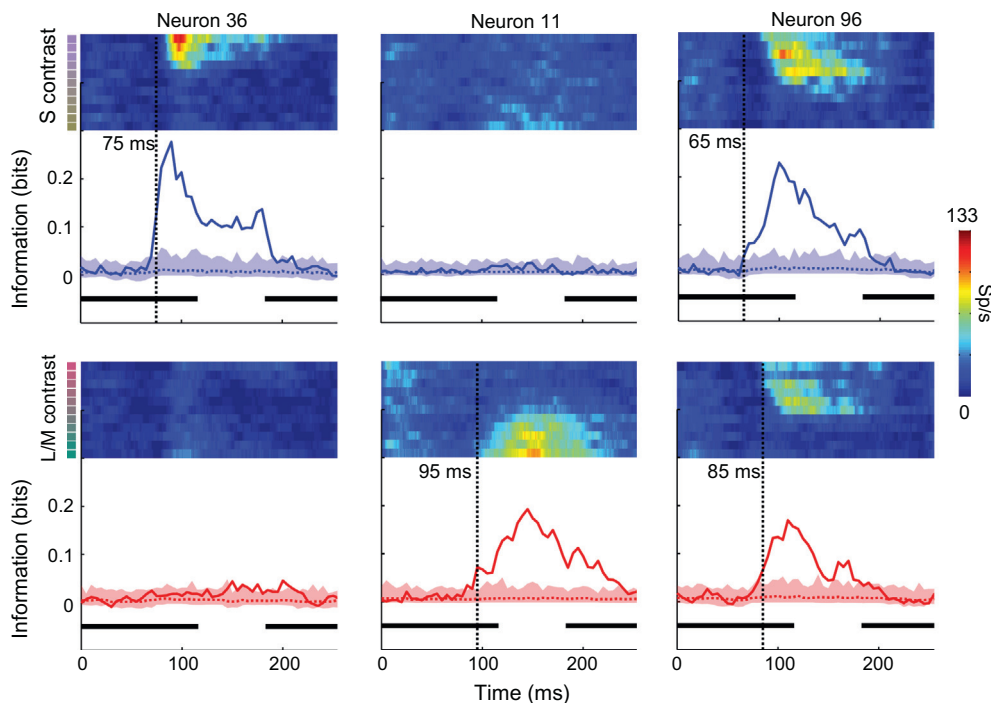


Fig. 2. Example PSTH and Information timecourses for S and L/M stimuli for three single neurons. Each column represents one example neuron, with timecourses of tuning and information for S stimuli (top, blue) and L/M stimuli (bottom, red). Heat maps correspond to the PSTH's, show the spike rate (color axis) in 15 ms bins across 11 colors along the S or L/M contrast axis (vertical axis) as a function of time (horizontal axis). Each information timecourse plot shows the bias-corrected MI (solid line) across time using the spike counts in 15 ms bins from the corresponding PSTH. Dotted curves with shading show the shuffled bootstrap MI values. Vertical dotted black lines indicate the estimated latency of the onset of information, using the first of 5 consecutive time points at which information exceeded the maximum of the shuffled bootstrapped values ($p < 0.01$ at each bin, corresponding to $p < 10^{-10}$ for 5 consecutive bins). Thick black lines under each curve indicate the duration of stimuli on the screen, and analyses were carried out with respect to the first stimulus.

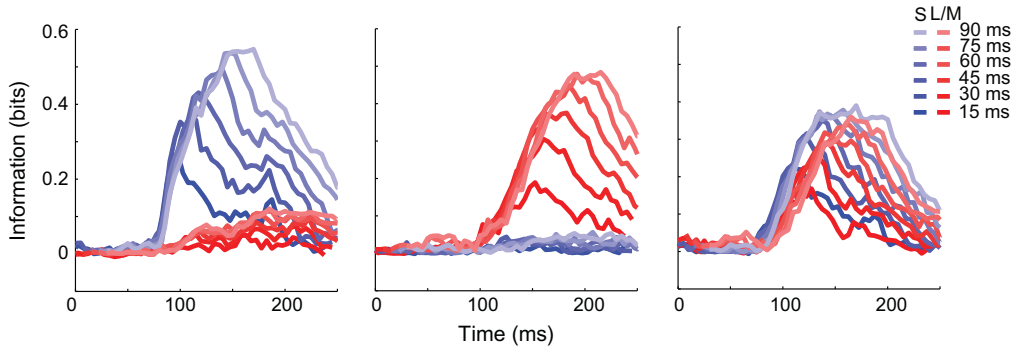


Fig. 3. Information timecourse for S and L/M contrast with varying time bins. MI timecourses for the same 3 example neurons as Fig. 2 are plotted using bin widths of 15, 30, 45, 60, 75, and 90 ms, aligned to the start of the bin.

responded most to positive S contrast (purplish) stimuli and was virtually unresponsive to neutral gray and colors with negative S-contrast (yellowish green) stimuli. This resulted in high selectivity for S contrast (one-way ANOVA, $p < 10^{-7}$).

Fig. 2 shows the average spiking responses and corresponding information along the S and L/M contrast axes for three example neurons: a neuron only selective for S contrast, a neuron only selective for L/M contrast, and a neuron selective for both. Note the first neuron (on the left) is the same as that depicted in Fig. 1. The peristimulus time histograms (PSTH) show spike rates as a function of color (vertical axis) and time (horizontal axis). Each vertical slice through the PSTH is the contrast tuning curve for the corresponding time point. We calculate the MI in a sliding window across time to quantify the association between the responses and the color stimuli. Below each PSTH is the corresponding MI timecourse, which appeared to closely follow the tuning observed in the PSTH, remaining near zero during the visual response latency and rising steeply or gradually according to the time at which responses diverged across contrasts. In the L/M-selective and both-selective example neurons, the onset of responses appeared to be faster for preferred contrasts, as observed in the staggered onset of activity across rows in the PSTH.

As a control, we examined the MI timecourse as a function of the width of the analysis window, shown in Fig. 3 for the same 3 example neurons. Note that the plots are aligned to the start of each bin rather than the center of each bin. Larger windows allow for a wider range of responses and better estimate of the firing rate, but lower time resolution. Latencies estimated from the short 15 ms analysis window did not differ significantly from the larger analysis windows (up to 90 ms).

To summarize the color selectivity of the population of recorded neurons, Fig. 4 shows a scatter plot of the maximum MI value reached for each neuron for S-contrast stimuli vs. L/M-contrast stimuli. Of the 255 recorded neurons, 89 neurons were significantly color-selective according to the latency measure criterion. Of the color-selective neurons, 24 were selective only for S contrast, 42 were selective only for L/M contrast, and 23 were selective for both. The maximum MI for S contrast and L/M contrast were comparable and not significantly different from each other (S median = 0.10, L/M median = 0.10, Wilcoxon rank sum, $p > 0.48$).

We then compared the latency of S contrast information in S-selective neurons with the latency of L/M contrast information in L/M-selective neurons. Fig. 5 shows a histogram of latencies for S and L/M contrast (right). On average, neurons showed comparable latencies in discriminating stimuli along both chromatic axes (S median latency = 95 ms, L/M median latency = 85 ms; Wilcoxon rank sum, $p > 0.3$). To the left of the histogram is a scatter plot of latencies for each contrast as a function of the maximum MI (left). The latency and maximum MI showed a strong correlation, as the

information timecourse for neurons that carried a low amount of information was such that the MI wavered near the shuffled bootstrap values, resulting in longer latencies to achieve the criterion of 5 consecutive time points above the bootstrapped values. This correlation was seen for both S-selective and L/M-selective neurons (S

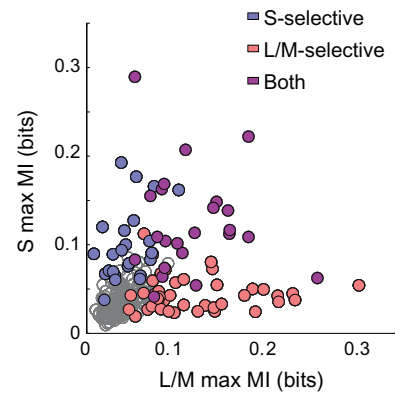


Fig. 4. S and L/M contrast information across a population. For each neuron, the maximum MI in a moving 15 ms analysis window for spiking responses to S contrast stimuli (y-axis) is plotted against the maximum MI for spiking responses to L/M contrast stimuli. Filled circles are colored based on selectivity for either or both contrast axes (blue for S-selective neurons, red for L/M selective neurons, and purple for neurons selective for both contrast axes), while grayed circles indicate neurons that did not carry significant information for either.

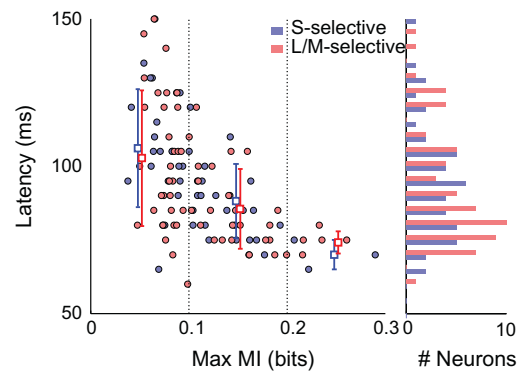


Fig. 5. Latency of S and L/M information across a population. Latency of S contrast information for neurons selective for L/M contrast (red) as a function of maximum MI. Note these represent overlapping populations of neurons. Mean latencies within each range of maximum MI (0–0.1, 0.1–0.2, 0.2–0.3) are shown as open squares (blue for S, red for L/M) with error bars depicting standard deviations. The histograms on the right show the distribution of latencies for S-selective and L/M-selective neurons.

correlation coefficient = -0.62 , $p < 10^{-5}$; L/M correlation coefficient = -0.55 , $p < 10^{-5}$). In order to compare latencies while taking into account the dependence on the amount of information, latencies were binned by the max MI (0–0.1, 0.1–0.2, and 0.2–0.3). Average latencies within each of these bins remained indistinguishable between S-selective and L/M selective neurons (Wilcoxon rank sum, $p > 0.3$).

4. Discussion

4.1. Convergence of S-opponent and L/M-opponent signal timing in extrastriate cortex

The results of this study suggest that on average, S-opponent and L/M-opponent signals arrive simultaneously in area V4. Mounting evidence suggests that the koniocellular pathway, which primarily carries S-cone signals, is distinct from the magno- and parvo-cellular projections from dLGN to cortex (Hendry and Reid, 2000), and appears to send direct projections to extrastriate cortex (including V2, V4, and MT) that bypass V1 (Lysakowski et al., 1988; Rodman et al., 2001; Sincich et al., 2004). This may provide an anatomical basis for the temporal convergence of S- and L/M-opponent signal despite the delay observed in V1, and these projections have also been implicated in cases of blindsight (Rodman et al., 2001).

Several psychophysical studies have examined temporal differences in the perception of cone contrast, opponent chromatic, and luminance signals, in a variety of pairwise comparisons. One study used a simple manual reaction time task to measure subjects' ability to detect the appearance of an equiluminant S-opponent or L/M-opponent signal and found that responses to S-opponent stimuli were slower by up to 300 ms depending on cone contrast, but these differences were reduced when detection threshold along each axis was taken into consideration (McKeefry et al., 2003). Another study used a manual reaction time task to measure subjects' ability to detect a S-opponent or L/M-opponent signal embedded within spatiotemporal luminance noise and found that reaction times to S-opponent signals were at most 20–30 ms slower than reactions to L/M opponent signals (Smithson and Mollon, 2004). However, the measured perceptual delay between S-cone contrast and luminance signals differed depending on whether the task required a manual response, a saccade, or a perceptual judgment of which stimulus appeared first (Bompas and Sumner, 2008). In this study, the average measured lag for S-cone signals was 23 ms for manual reactions and 44 ms for saccades, while no significant difference was observed for temporal order judgments. This suggests that the delays are introduced at later stages of processing, depending on the response modality. In another perceptual measure of S-cone sluggishness, a study found that when a blue and red bar were simultaneously swept across a yellow screen, subjects perceived the blue bar lagging behind the red bar, providing a perceptual measure of S-cone sluggishness (Mollon and Polden, 1976). However, after taking into account the adaptation of the background, the bars were perceived to be synchronous (Blake et al., 2008). These studies taken together suggest a weak basis for perceptual delays in S-cone stimuli and are consistent with the convergence of signal timing within area V4.

4.2. Measures of information

In the current study, spike count within a small time window was used as the basis for information. It is possible that additional information is contained in other features of the spike train. For example, many studies have considered the importance of the timing of the first flash following the stimulus onset (Bair and Koch,

1996; VanRullen et al., 2005). As observed in the PSTH's in Fig. 2, some neurons appear to respond more rapidly to preferred colors compared to non-preferred colors.

While the current results indicate a convergence of signal timing among chromatic channels, it would be interesting to see how this compares with the timing of achromatic signals, for example orientation. In the current experiment setup, it was not possible to examine latencies of orientation information because orientation was held constant across flashes within each trial. A possible solution would be to examine only the first flash within each trial, but since the colors were randomized and there were a limited number of trials relative to the number of colors, it was not plausible to examine only the first flash, controlled for color.

Acknowledgments

This work was supported by NIH Grant EY014924, NSF Grant IOB-0546891, the McKnight Endowment for Neuroscience, a Stanford Bio-X Bioengineering Graduate Fellowship, an NIH NRSA Grant F31NS062615, and a Siebel Scholarship (MHC). We thank D.S. Aldrich for technical assistance and S.A. Baccus for valuable comments on the analyses.

References

- Bair, W., Koch, C., 1996. Temporal precision of spike trains in extrastriate cortex of the behaving macaque monkey. *Neural Computation* 8, 1185–1202.
- Blake, Z., Land, T., Mollon, J., 2008. Relative latencies of cone signals measured by a moving vernier task. *Journal of Vision*, 8.
- Bompas, A., Sumner, P., 2008. Sensory sluggishness dissociates saccadic, manual, and perceptual responses: an S-cone study. *Journal of Vision*, 8.
- Chatterjee, S., Callaway, E.M., 2003. Parallel colour-opponent pathways to primary visual cortex. *Nature* 426, 668–671.
- Cole, G.R., Stromeyer, C.F., Kronauer, R.E., 1990. Visual interactions with luminance and chromatic stimuli. *Journal of the Optical Society of America A* 7, 128–140.
- Conway, B.R., Moeller, S., Tsao, D.Y., 2007. Specialized color modules in macaque extrastriate cortex. *Neuron* 56, 560–573.
- Cottaris, N.P., De Valois, R.L., 1998. Temporal dynamics of chromatic tuning in macaque primary visual cortex. *Nature* 395, 896–900.
- Cover, T., Thomas, J., 1991. *Elements of Information Theory*. Wiley and Sons.
- De Valois, R.L., Cottaris, N.P., Elfar, S.D., Mahon, L.E., Wilson, J.A., 2000. Some transformations of color information from lateral geniculate nucleus to striate cortex. *Proceedings of the National Academy of Sciences of the United States of America* 97, 4997–5002.
- Derrington, A.M., Krauskopf, J., Lennie, P., 1984. Chromatic mechanisms in lateral geniculate nucleus of macaque. *Journal of Physiology* 357, 241–265.
- Efron, B., 1979. Bootstrap methods: another look at the jackknife. *Annals of Statistics* 7, 1–26.
- Eskew Jr., R., Stromeyer, C., Kronauer, R., 1994. The time-course of chromatic facilitation by luminance contours. *Vision Research* 34, 3139–3144.
- Graziano, M.S.A., Hu, X.T., Gross, C.G., 1997. Visuospatial properties of ventral premotor cortex. *Journal of Neurophysiology* 77, 2268–2292.
- Hendry, S.H.C., Reid, R.C., 2000. The koniocellular pathway in primate vision. *Annual Review of Neuroscience* 23, 127–153.
- Hubel, D.H., Livingstone, M.S., 1987. Segregation of form, color, and stereopsis in primate area 18. *Journal of Neuroscience: The Official Journal of the Society for Neuroscience* 7, 3378–3415.
- Kotake, Y., Morimoto, H., Okazaki, Y., Fujita, I., Tamura, H., 2009. Organization of color-selective neurons in macaque visual area V4. *Journal of Neurophysiology* 102, 15–27.
- Livingstone, M.S., Hubel, D.H., 1984. Anatomy and physiology of a color system in the primate visual cortex. *Journal of Neuroscience: The Official Journal of the Society for Neuroscience* 4, 309–356.
- Logothetis, N., Charles, E., 1990. The minimum motion technique applied to determine isoluminance in psychophysical experiments with monkeys. *Vision Research* 30, 829–838.
- Lysakowski, A., Standage, G.P., Benevento, L.A., 1988. An investigation of collateral projections of the dorsal lateral geniculate nucleus and other subcortical structures to cortical areas V1 and V4 in the macaque monkey: a double label retrograde tracer study. *Experimental Brain Research* 69, 651–661.
- MacLeod, D.I.A., Boynton, R.M., 1979. Chromaticity diagram showing cone excitation by stimuli of equal luminance. *Journal of the Optical Society of America* 69, 1183–1186.
- McKeefry, D.J., Parry, N.R.A., Murray, I.J., 2003. Simple reaction times in color space: the influence of chromaticity, contrast, and cone opponency. *Investigative Ophthalmology & Visual Science* 44, 2267–2276.
- Mollon, J.D., Polden, P.G., 1976. Proceedings: some properties of the blue cone mechanism of the eye. *Journal of Physiology*, 254.

- Nelken, I., Chechik, G., 2007. Information theory in auditory research. *Hearing Research* 229, 94–105.
- Nelken, I., Chechik, G., Mrsic-Flogel, T.D., King, A.J., Schnupp, J.W., 2005. Encoding stimulus information by spike numbers and mean response time in primary auditory cortex. *Journal of Computational Neuroscience* 19, 199–221.
- Osborne, L.C., Bialek, W., Lisberger, S.G., 2004. Time course of information about motion direction in visual area MT of macaque monkeys. *Journal of Neuroscience: The Official Journal of the Society for Neuroscience* 24, 3210–3222.
- Panzeri, S., Treves, A., 1996. Analytical estimates of limited sampling biases in different information measures. *Network: Computation in Neural Systems* 7, 87–107.
- Rodman, H.R., Sorenson, K.M., Shim, A.J., Hexter, D.P., 2001. Calbindin immunoreactivity in the geniculo-extrastriate system of the macaque: implications for heterogeneity in the koniocellular pathway and recovery from cortical damage. *Journal of Comparative Neurology* 431, 168–181.
- Schmolesky, M.T., Wang, Y., Hanes, D.P., Thompson, K.G., Leutgeb, S., Schall, J.D., Leventhal, A.G., 1998. Signal timing across the macaque visual system. *Journal of Neurophysiology* 79, 3272–3278.
- Schnapf, J.L., Nunn, B.J., Meister, M., Baylor, D.A., 1990. Visual transduction in cones of the monkey *Macaca fascicularis*. *Journal of Physiology* 427, 681–713.
- Sincich, L.C., Horton, J.C., 2005. The circuitry of V1 and V2: integration of color, form, and motion. *Annual Review of Neuroscience* 28, 303–326.
- Sincich, L.C., Park, K.F., Wohlgenuth, M.J., Horton, J.C., 2004. Bypassing V1: a direct geniculate input to area MT. *Nature Neuroscience* 7, 1123–1128.
- Smith, V.C., Pokorny, J., 1975. Spectral sensitivity of the foveal cone photopigments between 400 and 500 nm. *Vision Research* 15, 161–171.
- Smithson, H.E., Mollon, J.D., 2004. Is the S-opponent chromatic sub-system sluggish? *Vision Research* 44, 2919–2929.
- Tailby, C., Solomon, S.G., Lennie, P., 2008. Functional asymmetries in visual pathways carrying S-cone signals in macaque. *Journal of Neuroscience* 28, 4078–4087.
- Tanigawa, H., Lu, H.D., Roe, A.W., 2010. Functional organization for color and orientation in macaque V4. *Nature Neuroscience* 13, 1542–1548.
- VanRullen, R., Guyonneau, R., Thorpe, S.J., 2005. Spike times make sense. *Trends in Neurosciences* 28, 1–4.
- Wiesel, T.N., Hubel, D.H., 1966. Spatial and chromatic interactions in the lateral geniculate body of the rhesus monkey. *Journal of Neurophysiology* 29, 1115–1156.
- Yeh, T., Lee, B.B., Kremersy, J., 1995. Temporal response of ganglion cells of the macaque retina to cone-specific modulation. *Journal of the Optical Society of America A* 12, 456–464.